

# UNIVERSITY OF MARYLAND



N56-5

## INSTITUTE FOR MOLECULAR PHYSICS

[REDACTED]

NONADDITIVITY OF INTERMOLECULAR FORCES: EFFECTS  
ON THE THIRD VIRIAL COEFFICIENT

[REDACTED]

A.E. Sherwood, Andrew G. De Rocco, and E.A. Mason

FACILITY FORM 902	N66 35316	
	(ACCESSION NUMBER)	(THRU)
	62	1
	(PAGES)	(COPIES)
	CD-68696	24
	(NASA CR OR TMX OR AD NUMBER)	(CATEGORY)

RECEIVED  
NOV 10 9 31 AM '65  
OFFICE OF GRANTS &  
RESEARCH CONTRACTS

GPO PRICE \$ \_\_\_\_\_

IMP-NASA-52

CFSTI PRICE(S) \$ \_\_\_\_\_

October 15, 1965

Hard copy (HC) 3.00

Microfiche (MF) .75

[REDACTED]

NONADDITIVITY OF INTERMOLECULAR FORCES: EFFECTS ON  
THE THIRD VIRIAL COEFFICIENT\*

A. E. Sherwood,<sup>†</sup> Andrew G. De Rocco, and E. A. Mason

Institute for Molecular Physics, University of Maryland  
College Park, Maryland

ABSTRACT


35316

The effects of nonadditive three-body forces on the third virial coefficient  $C(T)$  are examined. Corrections to the dispersion and repulsion pair potentials are taken, respectively, from third-order perturbation theory without exchange (triple-dipole) and from first-order perturbation theory with exchange. The repulsion is examined for two specialized models, a one-electron Gaussian model and an electrostatic distortion model. The results for the nonadditivity are shown to agree reasonably well with the quantum-mechanical results on one- and two-electron atoms. The magnitudes of the corrections to the repulsion and dispersion energies are of comparable magnitude but opposite sign for the ranges of interatomic separations of interest. Similarly, the correction to  $C(T)$  for repulsion nonadditivity is of opposite sign but

---

\* Supported in part by the U.S. National Aeronautics and Space Administration (Grant NSG-5-59).

<sup>†</sup> Present address: Lawrence Radiation Laboratory, Livermore, California.



comparable magnitude to that for dispersion nonadditivity in the temperature range of interest. The net correction, however, is of experimental significance, and it is suggested that careful experiments near the maximum in  $C(T)$  would be useful. The net correction to  $C(T)$  is unfortunately sensitive to the choice of the pair potential model, so that advances in knowledge of three-body forces from  $C(T)$  will probably depend on improvements first being made in knowledge of two-body forces.

## I. INTRODUCTION

One of the favorite simplifying assumptions of molecular physics is the pairwise additivity of the intermolecular potential. Although the nonadditive effects are often small, it has been known for some time that interesting phenomena are under their control; for example, polymorphism in the solid state.<sup>1</sup> Crystal properties, however, are not well suited for the study of nonadditive effects, because so many atoms or molecules interact simultaneously that the problem becomes very complicated.

The third virial coefficient, on the other hand, presents a theoretically simple and experimentally accessible property which depends on no more than the three-body interaction. It is perhaps the simplest case in which nonadditivity might be studied. Previous investigators have examined the nonadditivity of the long-range dispersion forces,<sup>2-5</sup> and its effect on the third virial coefficient.<sup>6-9</sup> No comparable study of the effect of nonadditivity of the short-range repulsive forces on the third virial coefficient has yet been made, but an indication has been given that the effects are not negligible.<sup>8</sup>

It is the purpose of this paper to investigate the influence of the three-body nonadditivity of the repulsive forces on the classical third virial coefficient.

In the following sections we first consider the theory of three-body forces for the purpose of formulating a reasonable model for the interaction of three atoms which includes non-additive contributions from both the attractive and the repulsive

components. We then use the model to study the behavior of the third virial coefficient as the components and parameters of the model are varied. It is found that the effects upon the third virial coefficient due to attractive and repulsive nonadditivity are of comparable magnitude but opposite sign in the temperature range of interest. Furthermore, the results are sensitive to the form assumed for the two-body potential.

## II. INTERMOLECULAR POTENTIAL MODEL

It is well to mention at the outset that the potentials used in molecular physics, even under the assumption of pairwise additivity, are really only models whose connection with fundamental theory is somewhat distant. In particular, the long-range pair potential is borrowed from second-order perturbation theory without exchange, and the short-range repulsive part of the pair potential is borrowed from first-order perturbation theory with exchange. Terms arising from second-order perturbation theory with exchange are commonly ignored, even though they are probably not negligible.<sup>10-13</sup> Various sins of omission and commission of this type are hopefully compensated by the use of adjustable parameters in the model.

It has been customary in computing nonadditive corrections to the third virial coefficient due to the long-range potential to include only the so-called triple-dipole term in the potential.<sup>6-9</sup> This corresponds to a third-order perturbation calculation without exchange. We propose to investigate the short-range potential to

obtain the nonadditive correction corresponding to a first-order calculation with exchange. Terms involving second-order exchange are ignored, just as in models of the pair potential, so that we write the total potential  $\varphi$  as

$$\varphi = \varphi_{\text{rep}} + \Delta\varphi_{\text{rep}} + \varphi_{\text{dis}} + \Delta\varphi_{\text{dis}}, \quad (1)$$

where  $\varphi_{\text{rep}}$  and  $\varphi_{\text{dis}}$  are the first-order short-range repulsion energy and the second-order long-range dispersion energy, respectively, and  $\Delta\varphi_{\text{rep}}$  and  $\Delta\varphi_{\text{dis}}$  are the nonadditive contributions. Many terms have been omitted from Eq.(1); to be consistent, the equation should probably include all terms through a third-order three-body exchange term.<sup>14</sup> Nevertheless, the terms included do give the correct asymptotic behavior at very small and very large separations. Most of the omitted terms probably make their main contributions at intermediate separations, and this can perhaps be allowed for by the use of adjustable parameters. In any event, it does not seem consistent to include second-order exchange terms in the nonadditive part of the potential unless corresponding terms are included in the pair potential.

The nonadditive second-order exchange energy appears to play a decisive role in the determination of the relative stability of the rare gas crystals,<sup>15</sup> whereas the additive second-order exchange energy does not. This cannot be construed as an argument to include such nonadditive terms in the present model, however, which is designed for the study of the third virial

coefficient. The reason is that it is only the relative crystal stability which has been investigated, and this depends explicitly on the angular dependence of the nonadditive second-order exchange energy, the additive part contributing essentially equally to the energies of both the hexagonal close-packed and the face-centered cubic structures. If the absolute value of the lattice energy were to be calculated, then it would be inconsistent to include the nonadditive contribution without the additive contribution as well, just as in the case of the third virial coefficient.

#### A. Dispersion Energy

We now briefly review the theory of the dispersion energy for later use. This energy can be computed either by a full quantum-mechanical treatment or by the use of a simple semi-classical picture of polarizable oscillators. In the latter treatment each atom is pictured as an oscillating dipole which induces an instantaneous dipole in its neighbor, and when averaged over time this mechanism leads to a net attraction of the form

$$\varphi_{\text{dis}} = - \frac{C}{R^6}, \quad (2)$$

where  $C$  is a constant and  $R$  is the interatomic separation. When three atoms are considered, the induced dipoles on the two neighbors interact with one another and produce a nonadditive

contribution of the form

$$\Delta \varphi_{\text{dis}} = \frac{\nu}{(R_{12}R_{13}R_{23})^3} (1 + 3 \cos \theta_1 \cos \theta_2 \cos \theta_3) , \quad (3)$$

where  $R_{ij}$  represents the separation of atoms  $i$  and  $j$ , and  $\theta_1$ ,  $\theta_2$ , and  $\theta_3$  are the interior angles of the triangle defined by the three atoms. Expressions of the same form as Eqs.(2) and (3) are obtained from the quantum-mechanical treatment.

It is clear that a relation should exist between  $\nu$  and  $C$  in terms of the properties of the atoms. The simple semiclassical picture does not give this relation very accurately,<sup>16</sup> but a quantum-mechanical treatment yields the result,<sup>3,6</sup>

$$\nu = \frac{3}{4} \alpha C , \quad (4)$$

where  $\alpha$  is the atomic polarizability.

### B. Repulsion Energy

A complete quantum-mechanical calculation of the repulsion energy nonadditivity is very difficult, and calculations have been carried out only for one- and two-electron atoms.<sup>17-19</sup> We therefore pass immediately to simplified pictures for this interaction.

#### 1. One-Electron Gaussian Model

Jansen<sup>14,15</sup> has shown how the quantum-mechanical results for one-electron atoms can be extended to many-electron atoms with



closed shells, by means of an effective one-electron model with a Gaussian charge distribution. The problem is then the same as for three hydrogen atoms with parallel electron spins, having atomic wave functions of the form

$$\psi(r) = (\beta^2/\pi)^{3/4} \exp(-\beta^2 r^2/2), \quad (5)$$

where  $\beta$  is an adjustable parameter and  $r$  is the distance of an electron from its nucleus. Jansen obtained an explicit expression for the first-order interaction energy of a three-atom system in an arbitrary configuration. The Gaussian model is appealing because all the necessary two- and three-center molecular integrals can be evaluated in closed form.<sup>20</sup> Even so, the final result is very cumbersome and will not be given here. A more useful result can be obtained by an asymptotic expansion of Jansen's expression for the case of a near-equilateral triangle with fairly large interatomic separations. The leading term of the nonadditive energy is

$$\begin{aligned} \Delta \varphi_{\text{rep}} = & -2 \Delta_{12} \Delta_{13} \Delta_{23} \left[ R_1^{-1}(23) + R_2^{-1}(13) + R_3^{-1}(12) \right. \\ & \left. - R_{12}^{-1} - R_{13}^{-1} - R_{23}^{-1} \right] + O(\Delta_{ij}^4) + \dots, \quad (6) \end{aligned}$$

where  $\Delta_{ij}$  is the overlap integral,

$$\Delta_{ij} = \exp(-\beta^2 R_{ij}^2/4), \quad (7)$$

$R_{ij}$  is the distance between atoms  $\underline{i}$  and  $\underline{j}$ , and  $R_i(jk)$  is the

distance between atom i and the midpoint of the line joining atoms j and k. In these expressions, all distances are measured in units of the Bohr radius  $a_0$ , and the energy is given in atomic units,  $e^2/a_0$ .

Equation (6) gives an accurate representation of Jansen's full expression for nearly equilateral triangles from large separations down to about  $0.8\sigma$ , where  $\sigma$  is the value of the separation for which the pair potential is zero,  $\varphi(\sigma) = 0$ . It is poorer at smaller separations, but here the nonadditive effects are less important because of the steep rise in the pair potential. Furthermore, the one-electron Gaussian model itself begins to fail at small separations, because of the increasing importance of multiple-exchange effects.<sup>14</sup> Equation (6) also describes the shape dependence of the repulsive nonadditivity reasonably well for triangles with no angle larger than 100 deg. It fails badly for nearly linear isosceles triangles, however, because the term  $R_{3(12)}^{-1}$  diverges in the asymptotic expansion. These shape effects are illustrated in Fig. 1, which was calculated at  $R = \sigma$  for argon ( $\beta = 0.33$ ,  $\beta\sigma = 2.1$ ). In the calculations of the third virial coefficient to follow, we shall argue that near-linear configurations are relatively unimportant in the integration over configurational phase space. The repulsive nonadditivity for such configurations can therefore be roughly set equal to zero, as shown by the dashed curve in Fig. 1, with little effect on the integration.

Equation (6) is still not in its most useful form, since it depends explicitly and sensitively on the Gaussian model.

It is better to use the Gaussian model only as a device for obtaining a relation between  $\Delta\varphi_{\text{rep}}$  and the pair potential. In other words, the ratio  $\Delta\varphi_{\text{rep}}/\varphi_{\text{rep}}$  would be expected to be less model-sensitive than either  $\Delta\varphi_{\text{rep}}$  or  $\varphi_{\text{rep}}$  alone. Such a situation exists for the dispersion energy, and is summarized by Eq.(4). An expansion of the full Gaussian model pair potential yields an asymptotic result analogous to Eq.(6),

$$\varphi_{\text{rep}} = \frac{\Delta^2}{R} \left[ 3 - \left( \frac{2}{\pi} \right)^{\frac{1}{2}} \left( \beta R + \frac{1}{\beta R} \right) \right] + O(\Delta^3) + \dots, \quad (8)$$

which is a good approximation to the full Gaussian result. It can also be used to point out a defect in the model; namely that  $\varphi_{\text{rep}}$  passes through zero at  $\beta R \approx 3.5$ , goes through a minimum, and then approaches zero asymptotically from below. This attractive region, spurious from the point of view of a first-order parallel-spin calculation, probably is a consequence of the approximate wave function used.

In the region of most interest for virial coefficient calculations, which turns out to be  $1.5 < \beta R < 2.5$ , the factor in brackets in Eq.(8) varies only from 1.7 to 0.7, so that it is a fair approximation to rewrite Eq.(8) as

$$\varphi_{\text{rep}} \approx \frac{\Delta^2}{R}. \quad (9)$$

As a quick check, for equilateral triangles Eqs. (6) and (9) yield

$$\frac{\Delta\varphi_{\text{rep}}}{\Sigma\varphi_{\text{rep}}} = -2 \left( \frac{2}{3^{\frac{1}{2}}} - 1 \right) \Delta, \quad (10)$$

which reveals a simple proportionality to the overlap integral. Rosen<sup>17</sup> found a similar proportionality in his quantum-mechanical calculations for three helium atoms, in which hydrogenic atomic wave functions were used.

The general combination of Eqs.(6) and (9) yields

$$\frac{\Delta \phi_{\text{rep}}}{\Sigma \phi_{\text{rep}}} = - 2 \frac{(\phi_{12}\phi_{13}\phi_{23})^{\frac{1}{2}}}{(\phi_{12}+\phi_{13}+\phi_{23})} (R_{12}R_{13}R_{23})^{\frac{1}{2}} \times \quad (11)$$

$$\times \left[ R_{1(23)}^{-1} + R_{2(13)}^{-1} + R_{3(12)}^{-1} - R_{12}^{-1} - R_{13}^{-1} - R_{23}^{-1} \right],$$

in which we have eliminated all  $\Delta_{ij}$  in favor of the corresponding  $\phi_{ij}$  by means of Eq.(9). For our virial coefficient calculations we wish to use the Lennard-Jones 12-6 and 9-6 pair potentials, which are

$$\phi(R) = 4\epsilon \left[ (\sigma/R)^{12} - (\sigma/R)^6 \right], \quad (12a)$$

$$\phi(R) = \frac{27}{4} \epsilon \left[ (\sigma/R)^9 - (\sigma/R)^6 \right], \quad (12b)$$

where  $\epsilon$  is the depth of the potential well and  $\phi(\sigma) = 0$ . For these potentials Eq.(11) takes the forms

$$\frac{\Delta \phi_{\text{rep}}}{\Sigma \phi_{\text{rep}}} = - 4(\epsilon^*)^{\frac{1}{2}} \frac{(R_{12}^* R_{13}^* R_{23}^*)^{-11/2}}{(R_{12}^{*-12} + R_{13}^{*-12} + R_{23}^{*-12})} \times$$

$$\times \left[ R_{1(23)}^{*-1} + R_{2(13)}^{*-1} + R_{3(12)}^{*-1} - R_{12}^{*-1} - R_{13}^{*-1} - R_{23}^{*-1} \right], \quad (13a)$$

$$\frac{\Delta\phi_{\text{rep}}}{\Sigma\phi_{\text{rep}}} = - (27\epsilon^*)^{\frac{1}{2}} \frac{(R_{12}^* R_{13}^* R_{23}^*)^{-4}}{(R_{12}^{*-9} + R_{13}^{*-9} + R_{23}^{*-9})} \times$$

$$\times \left[ R_{1(23)}^{*-1} + R_{2(13)}^{*-1} + R_{3(12)}^{*-1} - R_{12}^{*-1} - R_{13}^{*-1} - R_{23}^{*-1} \right], \quad (13b)$$

where  $R_{ij}^* = R_{ij}/\sigma$  and  $\epsilon^*$  is a dimensionless energy parameter,

$$\epsilon^* = \epsilon\sigma/e^2. \quad (14)$$

For comparison, the corresponding result for the dispersion energy for these pair potentials is

$$\frac{\Delta\phi_{\text{dis}}}{\Sigma\phi_{\text{dis}}} = \frac{3}{4} \alpha^* \frac{(1 + 3 \cos \theta_1 \cos \theta_2 \cos \theta_3)}{(R_{12}^* R_{13}^* R_{23}^*)^3 (R_{12}^{*-6} + R_{13}^{*-6} + R_{23}^{*-6})}, \quad (15)$$

where

$$\alpha^* = \alpha/\sigma^3 \quad (16)$$

is a dimensionless polarizability parameter.

The accuracy of the foregoing equations can be assessed by comparison with the results of complete quantum-mechanical calculations. This is done in Fig.2 for the case of three helium atoms arranged in an equilateral triangle, for which the calculations of Rosen<sup>17</sup> are available. Both Eq.(13a) and Eq.(13b) agree very well with Rosen's calculations; even Eq.(10) with  $\beta\sigma = 4.0$  agrees surprisingly well in view of the rather ruthless approximations made. Also shown in Fig.2 are some results for an

electrostatic distortion model, which is discussed in the next section.

A similar comparison is shown for helium, argon, and xenon at  $R=\sigma$  in Table I. The distortion model is poor for helium, but works reasonably well for the heavier gases. Also shown in Table I for comparison are the values of  $\Delta\varphi_{\text{dis}}/\Sigma\varphi_{\text{dis}}$  as calculated from Eq.(15). They are opposite in sign to  $\Delta\varphi_{\text{rep}}/\Sigma\varphi_{\text{rep}}$  but of comparable magnitude, and change by about the same ratio in going from helium to argon to xenon.

We turn now to a description of the distortion model and some discussion of its properties and utility.

## 2. Electrostatic Distortion Model

The motivation for this model is the Hellmann-Feynman electrostatic theorem,<sup>21</sup> which states that the forces on the nuclei of interacting atoms are given correctly by classical electrostatics, provided the correct electron probability distribution is known. The electron distribution is of course governed by quantum mechanics, not classical mechanics. The repulsion between two closed-shell atoms at small separations results from the quantum-mechanical distortion of the electron clouds from their original spherical symmetry. This distortion arises primarily from the Pauli exclusion principle.

The aim of this section is to concoct a simple model which will mimic the distortion of the electron clouds and which will still be mathematically tractable. Such a model can then be used

to calculate the full three-body repulsive interaction in terms of two-body interactions, just as the model of polarizable oscillators was used to calculate the three-body dispersion energy in Sec.IIA. Reasonable results can be hoped for if the model is used only to calculate relations among different interactions, and not to calculate any interaction energy in absolute terms.

The model we have used considers that the Pauli distortion displaces the centers of electronic charge from the atomic nuclei, and that this distortion can be described in first order by an electric dipole. The magnitudes and directions of the dipoles on the interacting atoms are of course related to each other, but the relation is complicated and has to be found by a detailed quantum-mechanical calculation of the charge distribution. This calculation is avoided by using the model to specify the distortion dipoles. It should be noted that the situation is not strictly analogous to the dipole model for the dispersion forces, where only one dipole need be specified and the others then follow by electrostatic induction. Here the problem is to determine the other dipoles when one dipole is specified, which can be done by making use of the known results for pair interactions.

Consider two interacting atoms 1 and 2 a distance  $R$  apart, with atom 1 having a specified distortion dipole of magnitude  $m_1$  at an angle  $\gamma_1$  with respect to the line of centers, as shown in Fig.3. A corresponding dipole exists in atom 2 of magnitude  $m_2$

and orientation angle  $\gamma_2$  related to  $\gamma_1$  by

$$\gamma_2 = \omega - \gamma_1, \quad (17)$$

where  $\omega$  is an unknown phase angle. We take  $m_2$  to be proportional to  $m_1$ , with the proportionality factor a function of  $R$ ,

$$m_2 = m_1 f(R). \quad (18)$$

The interaction energy of two coplanar dipoles is

$$\varphi(R) = m_1 m_2 R^{-3} (\sin \gamma_1 \sin \gamma_2 - 2 \cos \gamma_1 \cos \gamma_2), \quad (19)$$

so that the average repulsive interaction energy of atoms 1 and 2, obtained by averaging  $\gamma_1$  around  $2\pi$ , is

$$\varphi_{\text{rep}} = -\frac{3}{2} m_1^2 f(R) R^{-3} \cos \omega. \quad (20)$$

In order that the energy be repulsive we pick  $\pi/2 < \omega < 3\pi/2$ .

If we now equate this result to the repulsive term of some empirical pair potential, we can determine  $m_1$  and  $f(R)$ . For example, for the 12-6 potential we can write

$$m_1^2 = \frac{8\epsilon\sigma^3}{-3 \cos \omega}, \quad (21a)$$

$$f(R) = (\sigma/R)^9. \quad (21b)$$

Some of the  $R$  dependence could have been put into  $m_1$ , but this complication is not needed. For the 9-6 potential we write

$$m_1^2 = \frac{9\epsilon\sigma^3}{-2 \cos \omega}, \quad (22a)$$



$$f(R) = (\sigma/R)^6. \quad (22b)$$

It will also be convenient to take  $\omega = \pi$ .

We can now use these results to discuss the interaction of three atoms in an arbitrary configuration, as shown in Fig.4. Let us begin by calling atom 3 the specified, or "driving", dipole. The driver controls the instantaneous magnitudes and positions of the distortion dipoles of atoms 1 and 2 according to the rules obtained for pair interactions. It is obvious from Fig.4 that

$$\gamma_1 = \omega_1 + 2\theta_1 - \gamma_3, \quad (23a)$$

$$\gamma_2 = \omega_2 - 2\theta_2 - \gamma_3. \quad (23b)$$

The 1-3 pair or the 2-3 pair taken alone would give the previous pair potential when the dipole in 3 was rotated through  $2\pi$ . A nonadditive contribution arises from the interaction of the distortion dipoles in atoms 1 and 2, and is

$$\Delta\phi_{12} = \frac{1}{2} m_3^2 f(R_{13}) f(R_{23}) R_{12}^{-3} \cos 2\theta_3, \quad (24)$$

where the average over  $\gamma_3$  has been performed, and the phase angles have been chosen to assure that the sign agrees with the quantum-mechanical result for a triangular configuration.

Similar results can be obtained by letting atoms 1 and 2 in turn become the drivers, and since

$$\Delta\phi_{\text{rep}} = \frac{1}{3} (\Delta\phi_{12} + \Delta\phi_{13} + \Delta\phi_{23}), \quad (25)$$

we obtain the final result,

$$\frac{\Delta\varphi_{\text{rep}}}{\Sigma\varphi_{\text{rep}}} = \frac{1}{9} \frac{(f_{13}f_{23}R_{12}^{-3} \cos 2\theta_3 + f_{12}f_{23}R_{13}^{-3} \cos 2\theta_2 + f_{12}f_{13}R_{23}^{-3} \cos 2\theta_1)}{(f_{12}R_{12}^{-3} + f_{13}R_{13}^{-3} + f_{23}R_{23}^{-3})}, \quad (26)$$

where  $f_{ij} = f(R_{ij})$ . For equilateral triangles Eq.(26) reduces to

$$\frac{\Delta\varphi_{\text{rep}}}{\Sigma\varphi_{\text{rep}}} = -\frac{1}{18} f(R). \quad (27)$$

This is of the same sign and magnitude as the corresponding result for the Gaussian model, although the  $R$  dependence is somewhat different.

The shape dependence of  $\Delta\varphi_{\text{rep}}/\Sigma\varphi_{\text{rep}}$  for the distortion model is conveniently illustrated by picking an isosceles triangle configuration and using the 12-6 model for the pair potential. The result is

$$\frac{\Delta\varphi_{\text{rep}}}{\Sigma\varphi_{\text{rep}}} = \left(\frac{\sigma}{R}\right)^9 g(\theta), \quad (28)$$

where  $R$  is the length of one of the equal sides,  $\theta$  is the angle between these sides, and

$$g(\theta) = \frac{1}{9} \frac{(2 \sin \frac{1}{2}\theta)^{-3} \cos 2\theta - 2 (\sin \frac{1}{2}\theta)^{-9} \cos \theta}{(2 \sin \frac{1}{2}\theta)^{-12} + 2}. \quad (29)$$

This function is shown in Fig.5, where it can be seen that the result is in qualitative agreement with the quantum-mechanical calculations of Rosen and the Gaussian-model calculations of Jansen (shown in

Fig.1). At 60 deg the nonadditivity is negative and the total repulsion is therefore smaller than the sum of the pair potentials. At 180 deg, on the other hand, the nonadditivity is positive and the total repulsion is greater than the pairwise sum.

Other properties of the distortion model have already been discussed in connection with Table I. We now have two reasonable models for  $\Delta \phi_{\text{rep}}$ , the Gaussian and the distortion models, and can turn to an examination of the effect of nonadditivity on the third virial coefficient.

### III. NONADDITIVE CONTRIBUTIONS TO THE CLASSICAL THIRD VIRIAL COEFFICIENT

The third virial coefficient of gases is of particular interest because it involves the interaction of precisely three molecules. The coefficient can be formally written as the sum of two terms,  $C = C_{\text{add}} + \Delta C$ , where  $C_{\text{add}}$  is the value calculated under the assumption of additivity of pair potentials, and  $\Delta C$  is the correction due to nonadditivity, given by

$$\Delta C = -(8\pi^2 N_0^2 / 3) \iiint \exp (-\Sigma \phi_{ij} / kT) \times \\ \times \left[ \exp (-\Delta \phi / kT) - 1 \right] R_{12} R_{13} R_{23} dR_{12} dR_{13} dR_{23}, \quad (30)$$

where  $N_0$  is Avogadro's number. If  $\Delta \phi$  and hence  $\Delta C$  are not too large, it is possible to split  $\Delta C$  into dispersion and repulsion components by a two-variable Taylor series expansion in the

parameters characterizing the strengths of the nonadditive components of  $\Delta\phi$ . These parameters are  $\alpha^* = \alpha/\sigma^3$  for the dispersion and  $(\epsilon^*)^{1/2} = (\epsilon\sigma/e^2)^{1/2}$  for the Gaussian-model repulsion. The distortion-model repulsion has no strength parameter, but a dummy parameter can be inserted and later set equal to unity. This parameter can still be denoted as  $(\epsilon^*)^{1/2}$ . Keeping only the first two non-vanishing terms of the Taylor expansion, we obtain

$$\Delta C/b_o^2 \equiv \Delta C^* = \alpha^* \left( \frac{\partial \Delta C^*}{\partial \alpha^*} \right)_0 + (\epsilon^*)^{1/2} \left[ \frac{\partial \Delta C^*}{\partial (\epsilon^*)^{1/2}} \right]_0 + \dots, \quad (31)$$

where  $b_o = 2\pi N_o \sigma^3/3$ , and it is understood that the derivatives are to be evaluated at  $\alpha^* = 0$ ,  $\epsilon^* = 0$ .

Values of  $\alpha^*$  and  $\epsilon^*$  for the rare gases are given in Table II. Since they are small, it is expected that Eq.(31) will be accurate. This expectation is confirmed by the results exhibited in Table III, where  $\Delta C^*$  calculated by Eq.(31) is compared with  $\Delta C^*$  calculated by the full integral of Eq.(30), for some typical values of  $\alpha^*$  and  $\epsilon^*$ . The results from Eq.(31) are correct within 5% for the 12-6 potential and within 8% for the 9-6 potential.

#### A. Dispersion Nonadditivity

The long-range nonadditive dispersion contribution has previously been calculated for both the 12-6 and  $\infty$ -6 potentials.<sup>6-8</sup> We now compute the same quantity for the 9-6 potential. The nonadditive dispersion derivative for the 9-6 potential can be

written as

$$\left( \frac{\partial \Delta C^*}{\partial \alpha^*} \right)_0 = \frac{729}{4T^*} \int_0^\infty \int_{\frac{1}{2}}^1 \int_{1-y}^y \exp \left( - \sum \varphi_{ij}^* / T^* \right) \times \\ \times (1 + 3 \cos \theta \cos \theta_x \cos \theta_y) (xy)^{-2} (R^*)^{-4} dx dy dR^*, \quad (32)$$

where  $\varphi_{ij}^* = \varphi(R_{ij})/\epsilon$ ,  $T^* = kT/\epsilon$ , and the integration variables in Eq.(30) have been replaced by

$$xR^* = R_{12}/\sigma,$$

$$yR^* = R_{13}/\sigma,$$

$$R^* = R_{23}/\sigma.$$

The limits of integration are as shown in Fig.6.

The integral in Eq.(32) has been evaluated numerically by a computer program analogous to that used earlier for the 12-6 potential.<sup>8</sup> The numerical results are tabulated in Table IV, and are estimated to be accurate within 0.2% with respect to errors of truncation and interval size. The results are similar to those already noted for the 12-6 and  $\infty$ -6 potentials—the dispersion derivative is always positive and decreases with increasing temperature.

### B. Repulsion Nonadditivity

For an n-6 potential the nonadditive repulsion derivative can be written as

$$\left[ \frac{\partial \Delta C^*}{\partial (\epsilon^*)^{\frac{1}{2}}} \right]_0 = \frac{36}{T^*} \int_0^\infty \int_{\frac{1}{2}}^1 \int_{1-y}^y \exp \left( - \sum \varphi_{ij}^* / T^* \right) \times$$

$$\times g_n(x, y, R^*) xy (R^*)^5 dx dy dR^*. \quad (33)$$

The shape function  $g_n$  will vary according to which model is chosen for the repulsion nonadditivity. For the Gaussian model we have

$$g_n = - A_n (xy)^{(1-n)/2} (R^*)^{(1-3n)/2} \left[ d_{1(23)}^{-1} + d_{2(13)}^{-1} + d_{3(12)}^{-1} - x^{-1} - y^{-1} - 1 \right], \quad (34)$$

with

$$A_9 = (27)^{3/2}/4, \quad A_{12} = 16,$$

$$2d_{1(23)}^2 = x^2 + y^2 - \frac{1}{2},$$

$$2d_{2(13)}^2 = x^2 + 1 - \frac{1}{2} y^2,$$

$$2d_{3(12)}^2 = 1 + y^2 - \frac{1}{2} x^2.$$

For the distortion model we have

$$g_n = B_n (xy)^{-3} (R^*)^{3-2n} \left[ y^{6-n} \cos 2\theta_x + x^{6-n} \cos 2\theta_y + (xy)^{6-n} \cos 2\theta \right], \quad (35)$$

with

$$B_9 = 3/4, \quad B_{12} = 4/9.$$

An examination of  $g_n$  for the Gaussian model suggests difficulties in two limiting conditions: for  $x \rightarrow 0$  where  $x^{-1} \rightarrow \infty$ , and for  $x \rightarrow 1/2$  where  $d_{1(23)}^{-1} \rightarrow \infty$ . The limit  $x \rightarrow 0$  turns out

not to be troublesome, however, since this corresponds to a small separation of two molecules and the exponential factor makes this region of phase space essentially inaccessible. For  $x \rightarrow 0$  but  $xR^* \approx 1$ , i.e. large  $R^*$ , the integrand still will be damped out since  $g_n$  diminishes rapidly with increasing  $R^*$ . We avoid the region near  $x = 1/2$  by the arbitrary device of setting  $g_n = 0$  for  $d_{1(23)} \leq 0.4196$ , which corresponds to picking  $\theta \leq 100$  deg for isosceles triangles as was shown by the dashed curve in Fig.1. It has already been pointed out in connection with Fig.1 that the behavior of our approximate Gaussian model is unreasonable for nearly linear isosceles triangles, and that some kind of approximation is necessary. We choose 100 deg as the cutoff angle merely because this gives a reasonable approximation to the results for the full Gaussian model.

We have investigated the effect of varying the cutoff angle between 90 and 110 deg, and the results are indicated in Table V. The variation in the nonadditivity derivative relative to its value at 100 deg is about  $\pm 10\%$  for the 12-6 potential and about  $\pm 15\%$  for the 9-6 potential. We regard an uncertainty of this amount as tolerable, since the model itself is subject to the possibility of a larger error, even for nearly equilateral triangles.

The calculated values of the nonadditive repulsion derivative are tabulated in Table VI for the Gaussian and distortion models with the 9-6 and 12-6 potentials. Truncation and interval size errors are estimated to be less than a few

tenths of one percent. The large differences in the numerical values for the Gaussian and distortion models are only apparent; the values of  $(\epsilon^*)^{\frac{1}{2}}$  to be used in Eq.(31) are formally unity for the distortion model, but for the Gaussian model have values like those given in Table II. Even a cursory examination of the results in Table VI, and a comparison with those given in Table IV, shows that the repulsion and dispersion nonadditive effects tend to cancel each other.

#### IV. COMPARISON WITH EXPERIMENT

It is convenient to compare our results with one another and with experiment in terms of the Boyle parameters, introduced by Kihara<sup>22</sup> and further discussed by others.<sup>23</sup> Temperatures are measured in units of  $T_B$ , the temperature at which the second virial coefficient  $B$  is zero, and volumes are measured in units of the Boyle volume  $v_B$ ,

$$v_B = \left( T \frac{dB}{dT} \right)_{T_B} . \quad (36)$$

For a given pair potential,  $T_B$  and  $v_B$  are proportional to  $\epsilon$  and  $\sigma^3$ , respectively. The proportionality constants  $T_B^*$  and  $v_B^*$  are defined as

$$T_B^* = kT_B/\epsilon , \quad v_B^* = v_B/b_0 , \quad (37)$$

and are listed in Table VII for the 9-6, 12-6, and  $\infty$ -6 potentials.



For any particular substance the Boyle temperature and volume are independent of any assumed potential model, and are obtainable in principle from experimental measurements in the vicinity of the Boyle point. Since such measurements are seldom available, an alternative procedure is to fit experimental second virial coefficient data to an assumed potential and then compute  $T_B$  and  $v_B$  from the empirical parameters of the potential. The results of this procedure are not independent of the assumed potential, but are nearly so if the potential is sufficiently flexible to represent the data accurately. The Kihara core potential<sup>22</sup> is usually an adequate choice for this purpose, and in Table VIII are given the values of  $T_B^*$  and  $v_B^*$  for various spherical core sizes. From these results it is possible to obtain the values of the Boyle point properties of the rare gases given in Table IX. These are in good agreement with values given previously.<sup>22,23b</sup> It is of some interest to report that the use of the square-well potential instead of the Kihara core potential gives agreement with the values of Table IX to within 1% for all gases except krypton, for which the value of  $v_B$  differs by 2%.

The foregoing results have been used in drawing Fig.7, where the experimental third virial coefficients of the heavy rare gases (reduced by  $v_B^2$ ) are shown as a function of  $T/T_B$ , together with the curves calculated for the 9-6, 12-6, and  $\infty$ -6 potentials on the assumption of pairwise additivity. It is clear from this figure that the lower-temperature measurements lie well above the calculated two-body curves; this is especially true for

the  $\infty$ -6 potential, which also gives a poorer representation of second virial coefficients than the 9-6 or 12-6 potentials. From these results we conclude that nonadditivity corrections are necessary.

It is less clear that other features shown in Fig.7 are real effects which cannot be attributed to experimental error. Perhaps the most obvious of these is the greater steepness of the xenon data, but it would take only a 9% decrease in  $v_B$  to put the xenon data into sensible agreement with the other gases. In this connection it is worth mentioning that experimental virial coefficients are usually obtained from gas compressibility measurements by fitting a polynomial in the density to a pressure-density isotherm. The third virial coefficient is then the limiting curvature of the isotherm, and to expect an accuracy of even  $\pm 5\%$  in  $C(T)$  is perhaps optimistic, even for the most precise compressibility measurements.

To calculate nonadditive corrections we need values of  $\alpha^*$  and  $\epsilon^*$ ; these have already been given in Table II, as obtained from 12-6 potential parameters. A plot of these values is given in Fig.8, where it can be seen that  $(\epsilon^*)^{\frac{1}{2}}$  is approximately proportional to  $\alpha^*$ ,

$$(\epsilon^*)^{\frac{1}{2}} \approx K \alpha^*, \quad (38)$$

with  $K \approx 1.3$ . A relation of this sort is to be expected from the theory of the two-body dispersion energy and the definition of  $\epsilon^* = \epsilon\sigma/e^2$ . According to the simplified London theory, the

dispersion coefficient is<sup>21</sup>

$$C = 4\epsilon\sigma^6 \approx \frac{3}{4} \alpha^2 I, \quad (39)$$

where  $I$  is the atomic ionization energy. From this expression and that for  $\epsilon^*$  we find

$$K \approx \frac{1}{4} (3I\sigma/e^2)^{\frac{1}{2}}, \quad (40)$$

which is indeed nearly a constant, although somewhat less than 1.3.

If the values of  $\alpha^*$  and  $\epsilon^*$  given in Table II are even roughly correct, then deviations from the principle of corresponding states, such as suggested by the data in Fig.7, are not unexpected. However, for the sake of simplicity, and because our nonadditivity model is only approximate, we have based our numerical calculations on  $\alpha^* = 0.05$ , which is the average value for argon, krypton, and xenon. This choice implies  $(\epsilon^*)^{\frac{1}{2}} = 0.065$ , according to Eq.(38).

There is no reason to expect the nonadditivity parameters for the 9-6 and  $\infty$ -6 potentials to be the same as those for the 12-6 potential, any more than the two-body potential parameters are the same. It is not hard to find a relation among them, however, by matching the second virial coefficient curves at the Boyle point and using the results of Table VII, to yield

$$(\alpha^*)_{9-6} = 0.9(\alpha^*)_{12-6} = 0.045,$$

$$(\alpha^*)_{\infty-6} = 1.4(\alpha^*)_{12-6} = 0.070,$$

and

$$(\epsilon^*)_{9-6}^{\frac{1}{2}} = 0.9(\epsilon^*)_{12-6}^{\frac{1}{2}} = 0.0585.$$

We have taken  $(\epsilon^*)_{\infty-6} = 0$ , since we do not wish to make non-additivity corrections to a rigid sphere repulsion.

Results for the 9-6 potential are shown in Fig.9. The dispersion nonadditivity correction alone raises the calculated curve substantially above the experimental measurements. The repulsion nonadditivity correction lowers the calculated curve, but dominates over the dispersion correction to such an extent that the final corrected curve lies below the uncorrected pairwise additive curve, and is in poorer agreement with experiment. Both the Gaussian and the distortion models give essentially the same result for the repulsive nonadditivity correction.

Results for the 12-6 potential are shown in Fig.10, and differ conspicuously from the 9-6 results. Again the Gaussian and distortion models give agreement on the repulsion nonadditivity correction, and again the dispersion nonadditivity correction alone raises the calculated curve too much, but the net nonadditivity correction for both dispersion and repulsion now gives a final corrected curve which lies above the uncorrected pairwise additive curve, and which is in fairly good agreement with experiment.

For the sake of completeness, results for the  $\infty$ -6 potential are shown in Fig.11. It is clear that this potential,

while simple enough, is of only marginal value in studies of empirical potential energy curves.

## V. CONCLUSIONS

In this study we have employed two approximate models for the nonadditivity of the three-body repulsion potential, to study the effect of repulsion nonadditivity on the third virial coefficient. The two models give surprisingly similar results for the third virial coefficient. Without attributing too much significance to the models themselves, we feel that the calculations justify two main conclusions:

(1) The correction to the third virial coefficient for repulsion nonadditivity is of opposite sign but comparable magnitude to that for dispersion nonadditivity, and the magnitude of the net correction is of experimental significance.

(2) The nonadditivity corrections are sensitive to the choice of the pair potential model.

The following third conclusion is probably also justified:

(3) The nonadditive effects are most pronounced at low temperatures; accurate experimental values of  $C(T)$  in the region of the maximum would consequently be very helpful in furthering our knowledge of the three-body forces.

From these conclusions several inferences can be drawn, as follows:

(1) No existing models are capable of giving reliable information on three-body forces.

(2) Advances in our knowledge of three-body forces are probably contingent on improvements in our knowledge of two-body forces, especially repulsion.

(3) At present, approximate models can serve only as guides to the direction a proper theory should take.

#### ACKNOWLEDGMENTS

The numerical calculations were carried out by the University of Maryland Computer Science Center. This computer time was supported by National Aeronautics and Space Administration Grant NsG-398 to the Computer Science Center. One of us (A.G. De R) wishes to thank the General Research Board of the University of Maryland for a grant which helped to support this work.

Table I. Comparison of the relative nonadditive energy for helium, argon, and xenon in an equilateral configuration at  $R=\sigma$ .

$\Delta\phi_{\text{rep}}/\Sigma\phi_{\text{rep}}$			
Model	Helium	Argon	Xenon
Rosen	- 0.0098	-	-
Gaussian-12	- 0.0077	- 0.031	- 0.046
Gaussian-9	- 0.0090	- 0.036	- 0.054
Distortion-12	- 0.0556	- 0.056	- 0.056
Distortion-9	- 0.0556	- 0.056	- 0.056
$\Delta\phi_{\text{dis}}/\Sigma\phi_{\text{dis}}$			
Oscillator	+ 0.0041	+ 0.013	+ 0.020

Table II. Nonadditivity parameters for the rare gases, based on 12-6 potential parameters.

Substance	$\alpha^*$	$(\epsilon^*)^{\frac{1}{2}}$
He <sup>a</sup>	0.012	0.012
Ne <sup>b</sup>	0.018	0.025
Ar <sup>c</sup>	0.038	0.050
Kr <sup>c</sup>	0.044	0.061
Xe <sup>c</sup>	0.058	0.074

<sup>a</sup> Reference 21.

<sup>b</sup> Obtained by fitting second virial data:  
 $\epsilon/k = 36.1^\circ\text{K}$ ,  $\sigma = 2.774 \text{ \AA}$ .

<sup>c</sup> A. E. Sherwood and J. M. Prausnitz, J. Chem. Phys. 41, 429(1964).



Table III. Comparison of the full nonadditivity integral for  $C^*$  with the derivative approximation of Eq.(31).

$\frac{kT}{\epsilon}$	12-6 potential $\alpha^* = 0.05, (\epsilon^*)^{\frac{1}{2}} = 0.065$		9-6 potential $\alpha^* = 0.045, (\epsilon^*)^{\frac{1}{2}} = 0.0585$	
	Integral	Eq. (31)	Integral	Eq. (31)
0.5	4.54	4.62	-11.96	-11.00
1.0	0.433	0.439	-0.553	-0.515
2.0	0.115	0.117	-0.0959	-0.0879
5.0	0.0311	0.0321	-0.0344	-0.0317
10.0	0.0116	0.0112	-0.0255	-0.0240

Table IV. The nonadditive dispersion derivative for the 9-6 potential.

$T^*$	$\left(\frac{\partial \Delta C^*}{\partial \alpha^*}\right)_0$
0.50	463.014
0.55	283.428
0.60	188.585
0.65	133.708
0.70	99.604
0.75	77.164
0.80	61.697
0.85	50.620
0.90	42.427
0.95	36.200
1.00	31.358
1.05	27.515
1.10	24.411
1.15	21.867
1.20	19.752
1.25	17.974
1.30	16.462
1.35	15.165
1.40	14.042
1.45	13.062
1.50	12.202
1.60	10.764
1.70	9.615
1.80	8.679
1.90	7.903
2.00	7.252
2.20	6.222
2.40	5.446
2.60	4.843
2.80	4.362
3.00	3.970
3.20	3.644
3.40	3.369
3.60	3.135
3.80	2.932
4.00	2.755
5.00	2.128
6.00	1.745
10.00	1.047
100.00	0.157

Table V. Effect of variation in cutoff angle on the values of the repulsion nonadditivity derivative for the approximate Gaussian model.

T*	Cutoff angle, deg	$-\left[\partial\Delta C^*/\partial(\epsilon^*)^{\frac{1}{2}}\right]_0$	
		9-6	12-6
1.0	90	28.2	5.09
	100	32.9	5.65
	110	36.8	6.04
5.0	90	1.77	0.355
	100	2.18	0.413
	110	2.55	0.458

Table VI. Nonadditive repulsion derivative for the 9-6 and 12-6 potentials.

T*	$\left[ \partial \Delta C^* / \partial (\epsilon^*)^{\frac{1}{2}} \right]_0$			
	Approx. Gaussian Model		Distortion Model ( $\epsilon^* = 1$ )	
	9-6	12-6	9-6	12-6
0.50	-544.242	-96.539	-29.182	-7.161
0.55	-328.646	-57.934	-17.663	-4.364
0.60	-215.754	-37.830	-11.623	-2.890
0.65	-150.991	-26.354	-8.153	-2.039
0.70	-111.083	-19.313	-6.013	-1.512
0.75	-85.045	-14.738	-4.615	-1.167
0.80	-67.246	-11.621	-3.658	-0.929
0.85	-54.600	-9.415	-2.977	-0.760
0.90	-45.322	-7.800	-2.477	-0.636
0.95	-38.325	-6.587	-2.100	-0.541
1.00	-32.924	-5.652	-1.808	-0.468
1.05	-28.669	-4.917	-1.579	-0.411
1.10	-25.257	-4.330	-1.394	-0.364
1.15	-22.479	-3.852	-1.244	-0.326
1.20	-20.185	-3.458	-1.120	-0.295
1.25	-18.269	-3.130	-1.016	-0.269
1.30	-16.650	-2.853	-0.928	-0.247
1.35	-15.269	-2.618	-0.853	-0.228
1.40	-14.080	-2.415	-0.788	-0.211
1.45	-13.049	-2.240	-0.732	-0.197
1.50	-12.148	-2.087	-0.683	-0.185
1.60	-10.654	-1.833	-0.602	-0.164
1.70	-9.472	-1.633	-0.538	-0.148
1.80	-8.518	-1.472	-0.486	-0.134
1.90	-7.734	-1.340	-0.443	-0.124
2.00	-7.081	-1.230	-0.407	-0.114
2.20	-6.058	-1.058	-0.351	-0.100
2.40	-5.299	-0.931	-0.310	-0.090
2.60	-4.715	-0.833	-0.278	-0.081
2.80	-4.254	-0.756	-0.252	-0.075
3.00	-3.882	-0.694	-0.232	-0.070
3.20	-3.575	-0.643	-0.215	-0.065
3.40	-3.318	-0.601	-0.201	-0.062
3.60	-3.100	-0.565	-0.189	-0.059
3.80	-2.912	-0.534	-0.179	-0.056
4.00	-2.750	-0.507	-0.170	-0.054
5.00	-2.179	-0.413	-0.138	-0.046
6.00	-1.836	-0.356	-0.119	-0.041
10.00	-1.216	-0.256	-0.085	-0.033
100.00	-0.369	-0.122	-0.039	-0.028

Table VII. Reduced Boyle temperatures and volumes for the 9-6, 12-6, and  $\infty$ -6 potentials.

Potential	$T_B^*$	$v_B^*$
9-6 <sup>a</sup>	4.5553	0.7153
12-6 <sup>b</sup>	3.4179	0.8113
$\infty$ -6 <sup>c</sup>	1.1709	1.1738

<sup>a</sup> L.F. Epstein and C.J. Hibbert, J. Chem. Phys. 20, 752(1952).

<sup>b</sup> Reference 21, pp.1114-1115.

<sup>c</sup> A.E. Sherwood and J.M. Prausnitz, J. Chem. Phys. 41, 429(1964).

Table VIII. Reduced Boyle temperatures and volumes for the Kihara core potential.

$a^*$ <sup>a</sup>	$T_B^*$	$v_B^*$
0.	3.418	0.8112
0.025	3.265	0.8255
0.050	3.126	0.8391
0.075	2.998	0.8523
0.100	2.880	0.8649
0.125	2.772	0.8771
0.150	2.671	0.8888
0.175	2.578	0.9002
0.200	2.491	0.9112
0.225	2.410	0.9219
0.250	2.335	0.9323
0.275	2.264	0.9424
0.300	2.198	0.9522
0.350	2.077	0.9711
0.400	1.970	0.9892
0.450	1.874	1.0065
0.500	1.788	1.0231
0.550	1.711	1.0392
0.600	1.641	1.0546
0.650	1.577	1.0697
0.700	1.518	1.0842
0.750	1.464	1.0984
0.800	1.415	1.1123
0.850	1.369	1.1258

<sup>a</sup> The reduced core  $a^*$  is defined as  $a^* = \frac{2a}{\sigma - 2a}$ , where  $a$  is the core radius. Note that  $a^* = 0$  corresponds to a 12-6 potential.

Table IX. Calculated Boyle point properties for the rare gases.

Substance	$T_B(^{\circ}\text{K})$	$v_B(\text{cc/mole})$
Ne	123	21.8
Ar	408	40.3
Kr	576	49.0
Xe	770	66.2

Fig. 1 - Effect of configuration on the first-order nonadditive repulsion energy for the one-electron Gaussian model and its asymptotic expansion, Eq.(6).



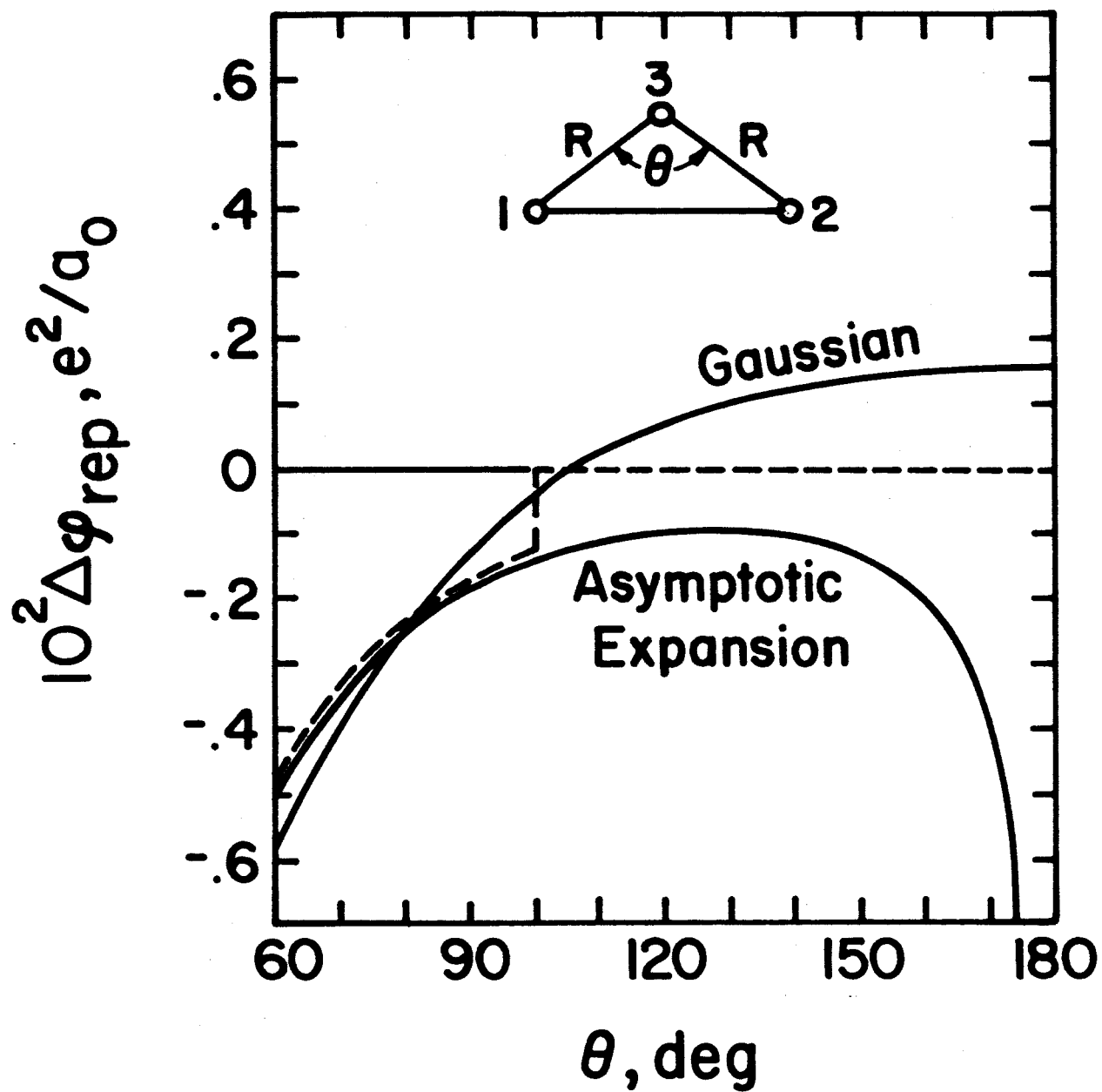
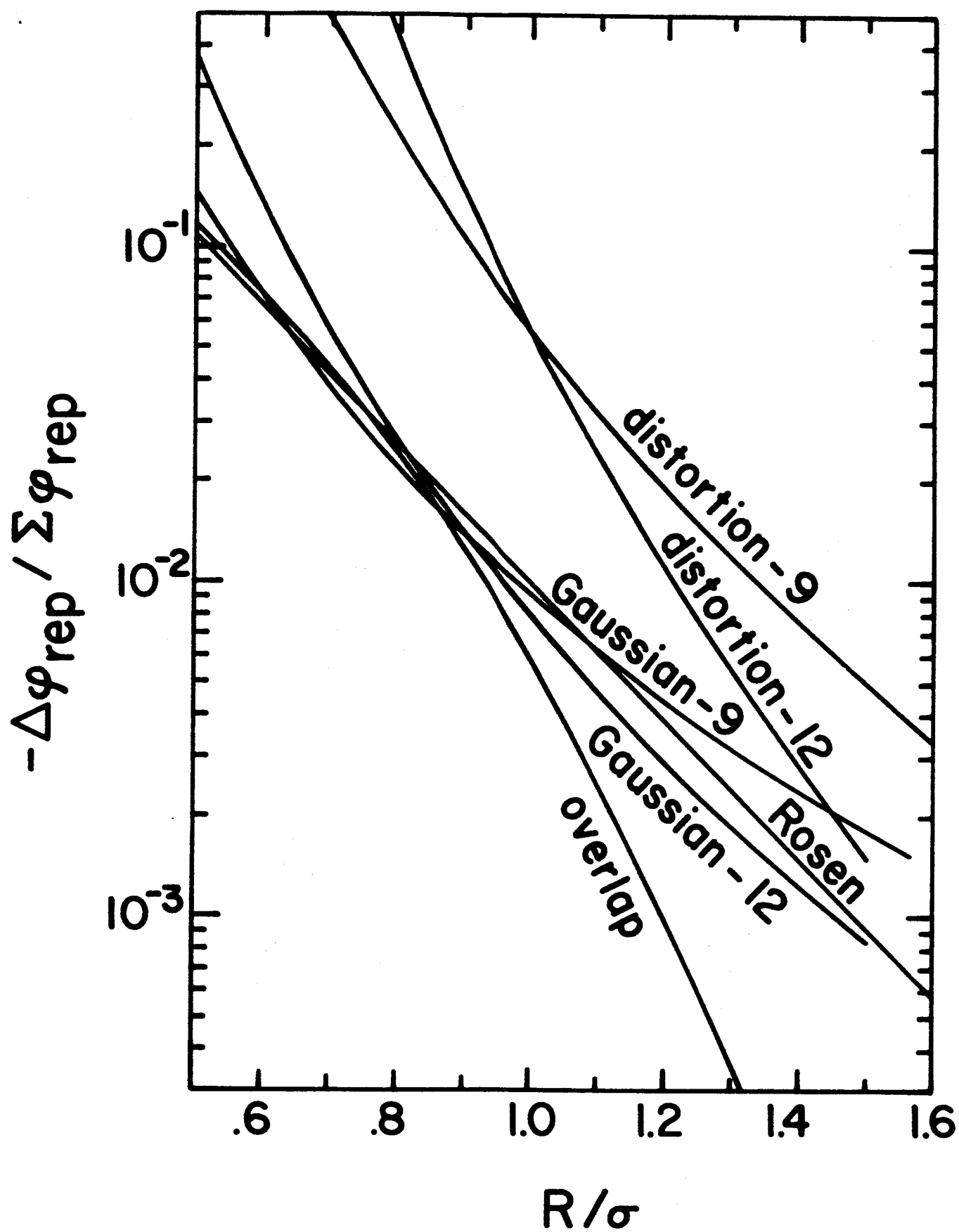
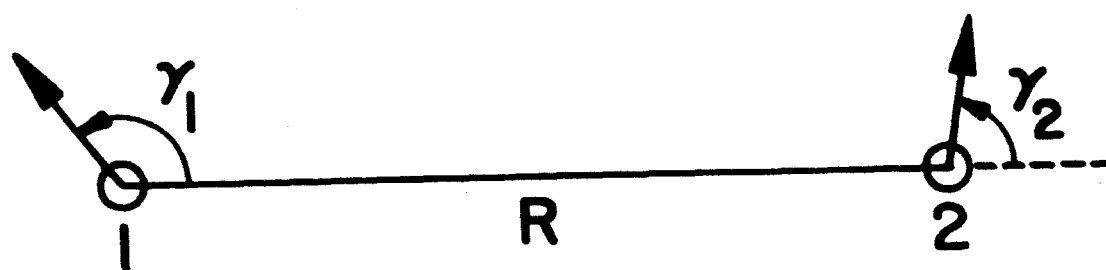


Fig. 2 - Comparison of different calculations of the first-order nonadditive repulsion energy for three helium atoms in an equilateral-triangle configuration. The curve marked "overlap" comes from Eq.(10); the curves marked "Gaussian-12" and "Gaussian-9" come from Eqs.(13a) and (13b); the curves marked "distortion-12" and "distortion-9" come from Eq.(26).



**Fig. 3 - Configuration of two distortion dipoles  
used to calculate the repulsion energy.**



**Fig. 4 - Configuration of three atoms and their instantaneous distortion dipoles, chosen for the calculation of the repulsion nonadditivity.**

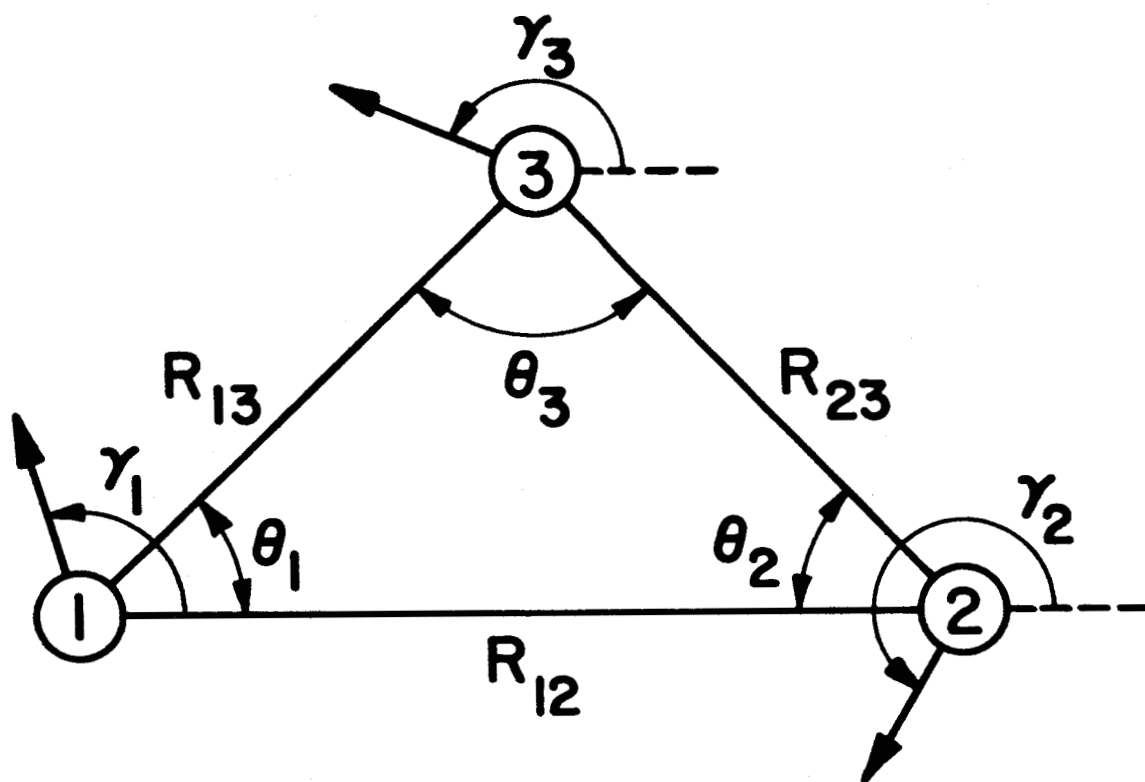


**Fig. 5 - Configuration dependence of the non-additive repulsion energy for the distortion model.**



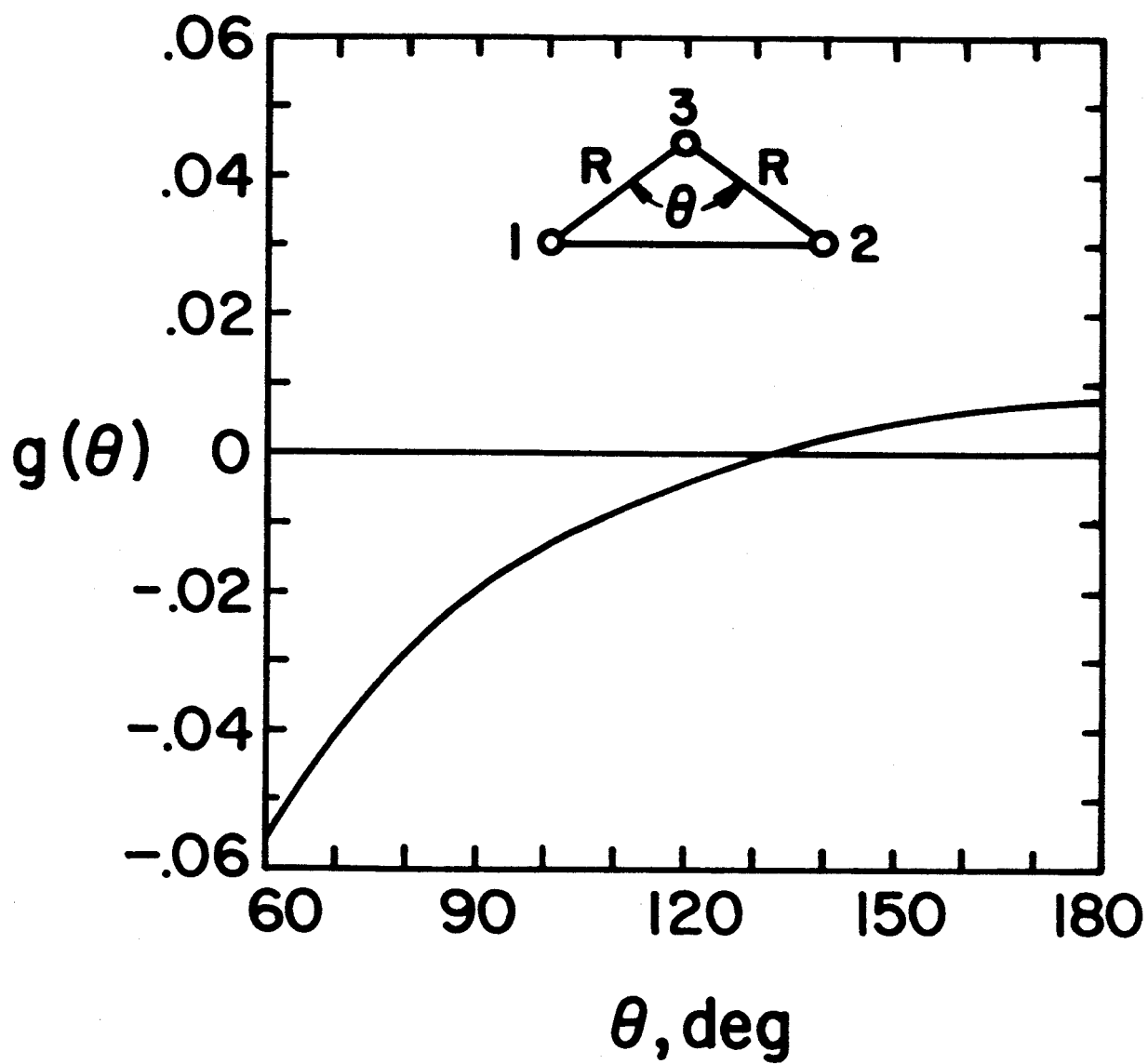


Fig. 6 - Region of integration for the third virial coefficient. Solid lines enclose the region in which molecule 1 is restricted to move for a given separation  $R^*$  of 2 and 3, consistent with  $x \leq y \leq 1$ .

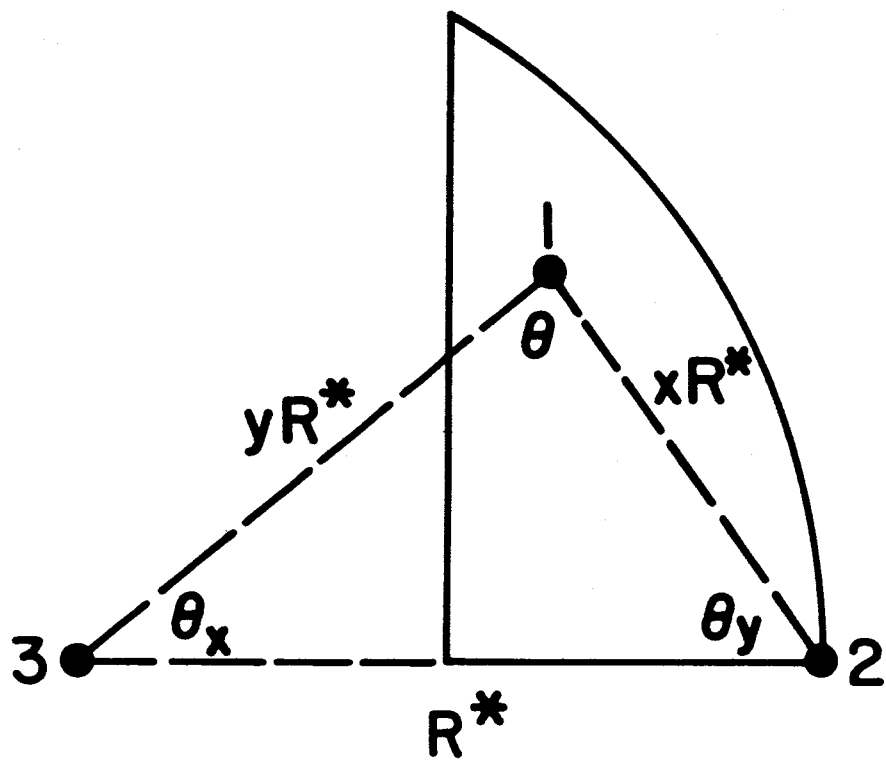


Fig. 7 - Reduced third virial coefficients for the rare gases, and calculated two-body curves for the 9-6, 12-6, and  $\infty$ -6 potentials. Experimental data from the following sources.

Neon,  $\odot$ : A. Michels, T. Wassenaar, and  
P. Louwerse, *Physica* 26, 539(1960).

Argon,  $\circ$ : A. Michels, Hub. Wijker, and Hk.  
Wijker, *Physica* 15, 627(1949); A  
Michels, J.M.H. Levelt, and  
W. de Graaff, *Physica* 24, 659(1958).

Krypton,  $\Delta$ : J.A. Beattie, J.S. Brierley, and  
R.J. Barriault, *J. Chem. Phys.* 20,  
1615(1952).

Xenon,  $\square$ : J.A. Beattie, R.J. Barriault, and  
J.S. Brierley, *J. Chem. Phys.* 19,  
1222(1951).

Xenon,  $\blacksquare$ : A. Michels, T. Wassenaar, and P.  
Louwerse, *Physica* 20, 99(1954).

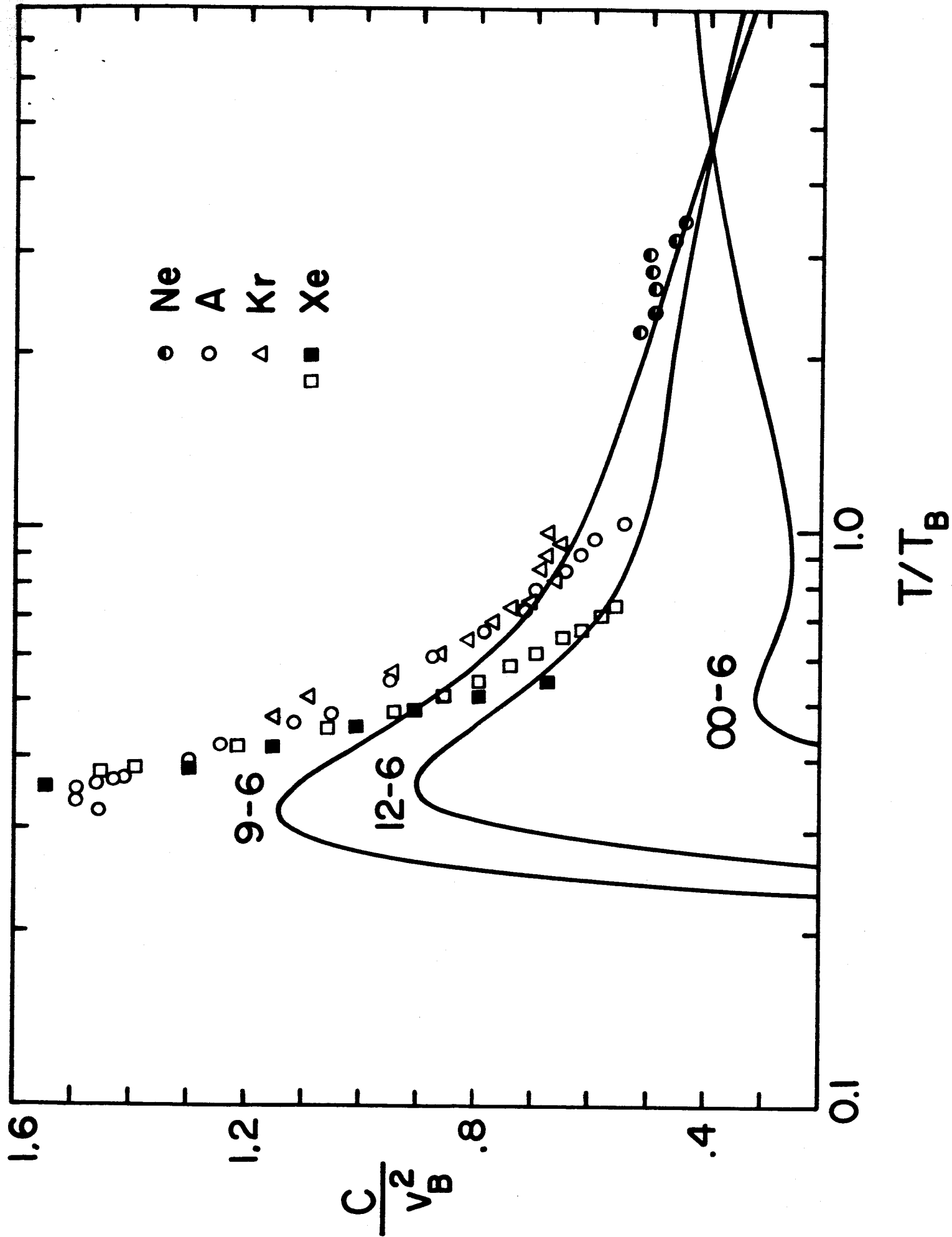
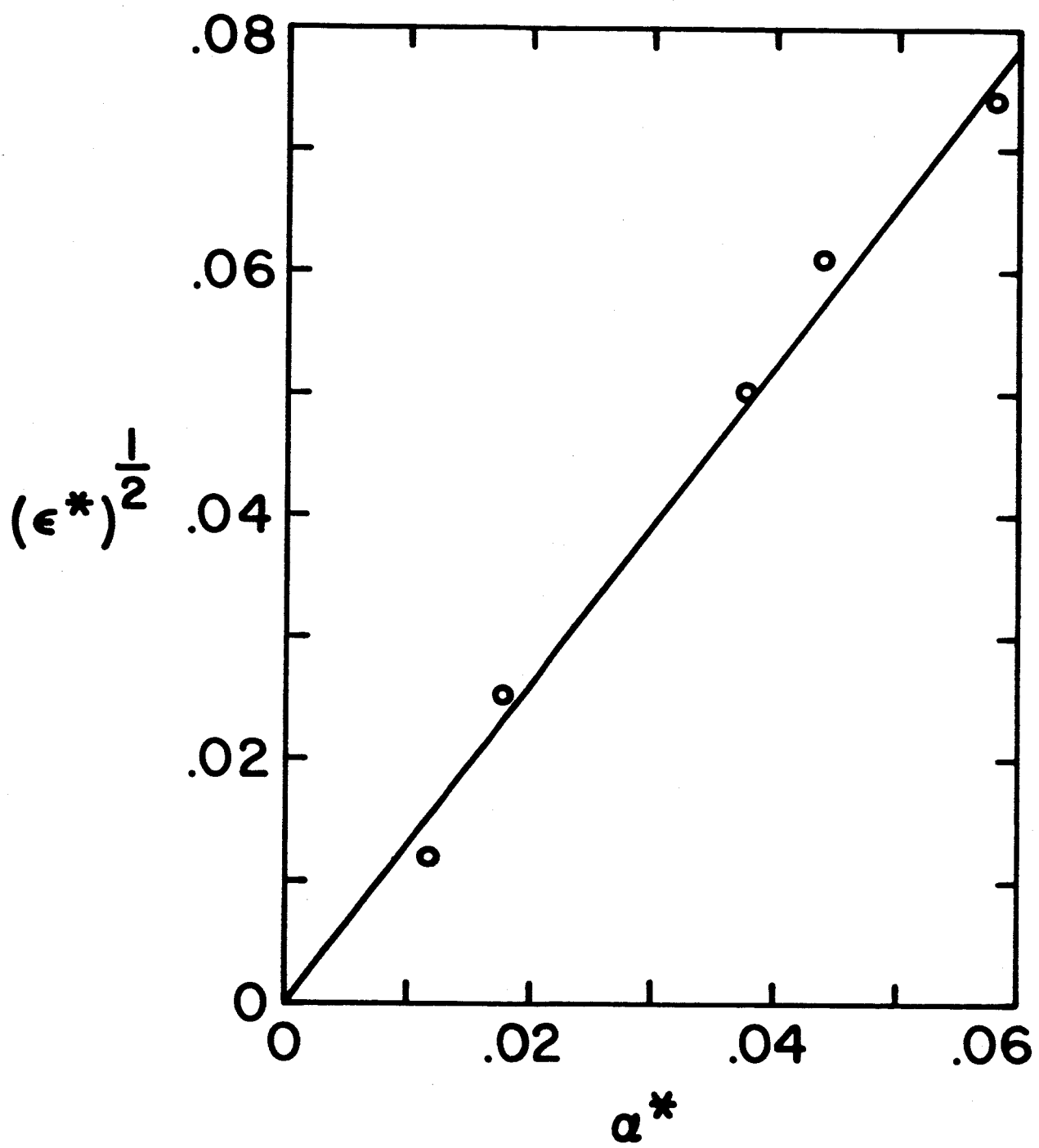


Fig. 8 - Nonadditivity parameters for the rare gases; repulsion,  $(\epsilon^*)^{\frac{1}{2}}$ , as a function of dispersion,  $\alpha^*$ , based on 12-6 potential parameters.



**Fig. 9 - Reduced third virial coefficient for the 9-6 potential.**

**Curve 1: Pairwise additive**

**Curve 2: Additive plus dispersion nonadditivity**

**Curve 3: Additive plus dispersion nonadditivity  
plus repulsion nonadditivity (Gaussian  
model)**

**Curve 4: Additive plus dispersion nonadditivity  
plus repulsion nonadditivity (dis-  
tortion model)**

**Experimental points as in Fig. 7**



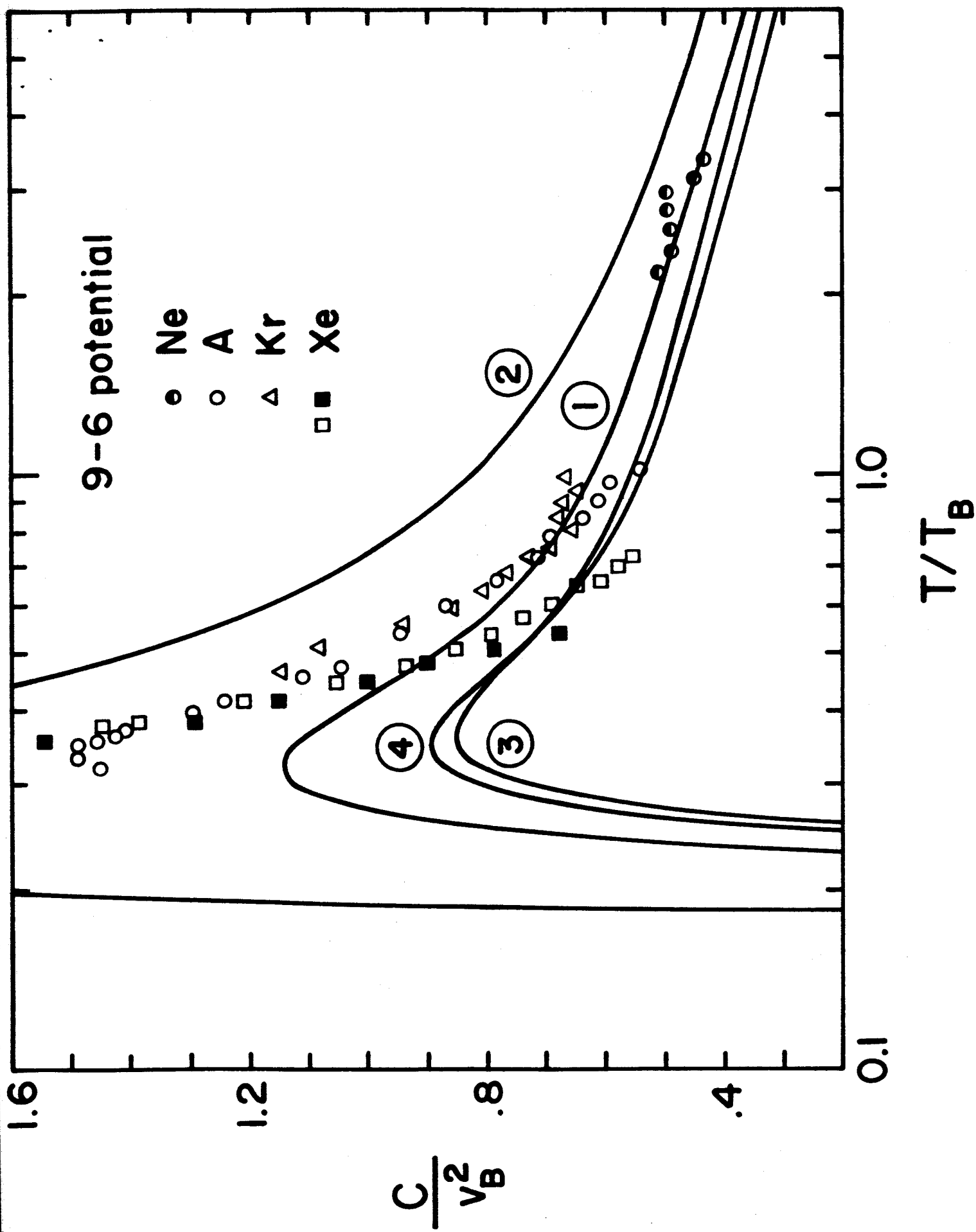


**Fig. 10 - Reduced third virial coefficient for the  
12-6 potential. Labeling of curves and  
experimental points as in Fig.9.**

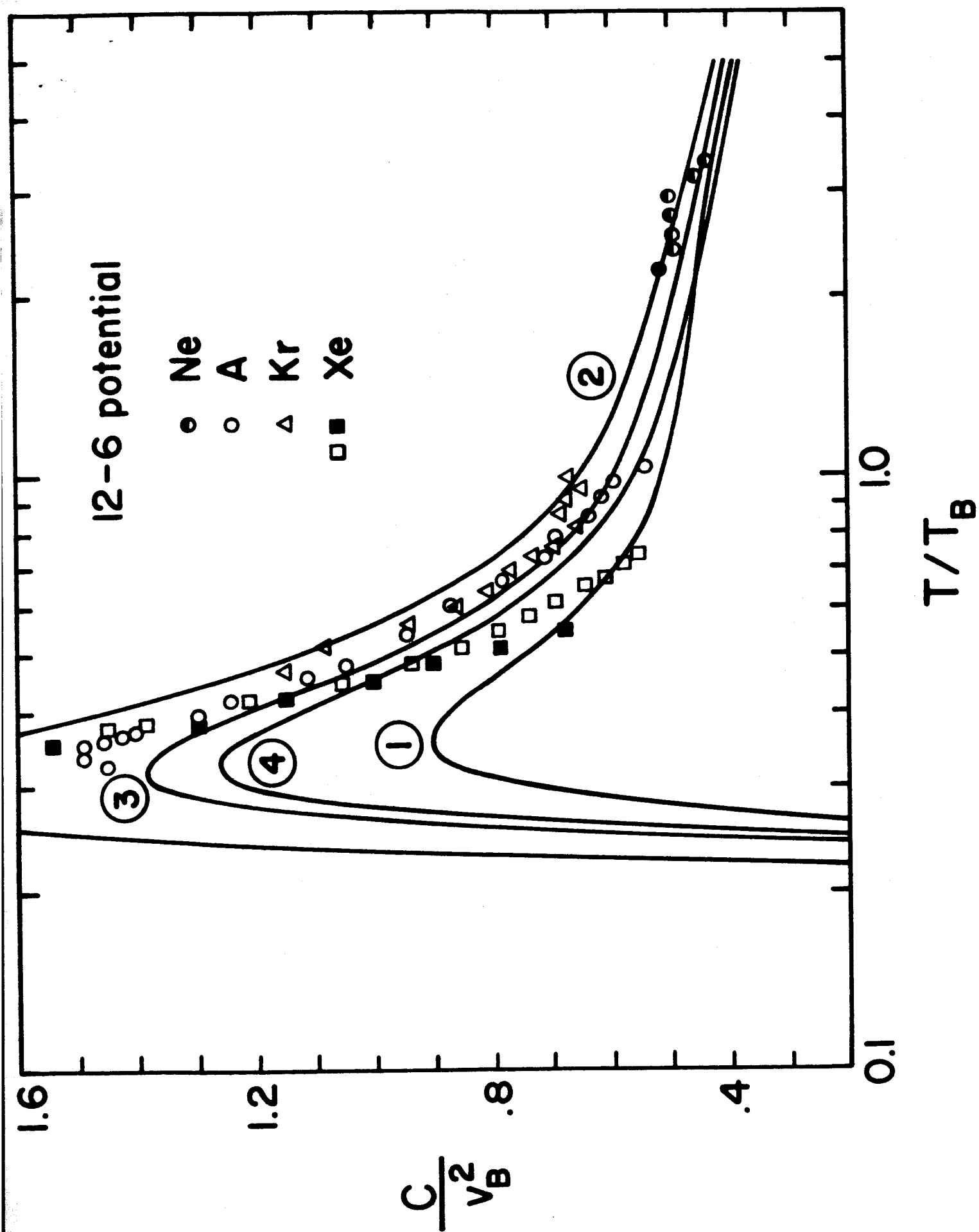
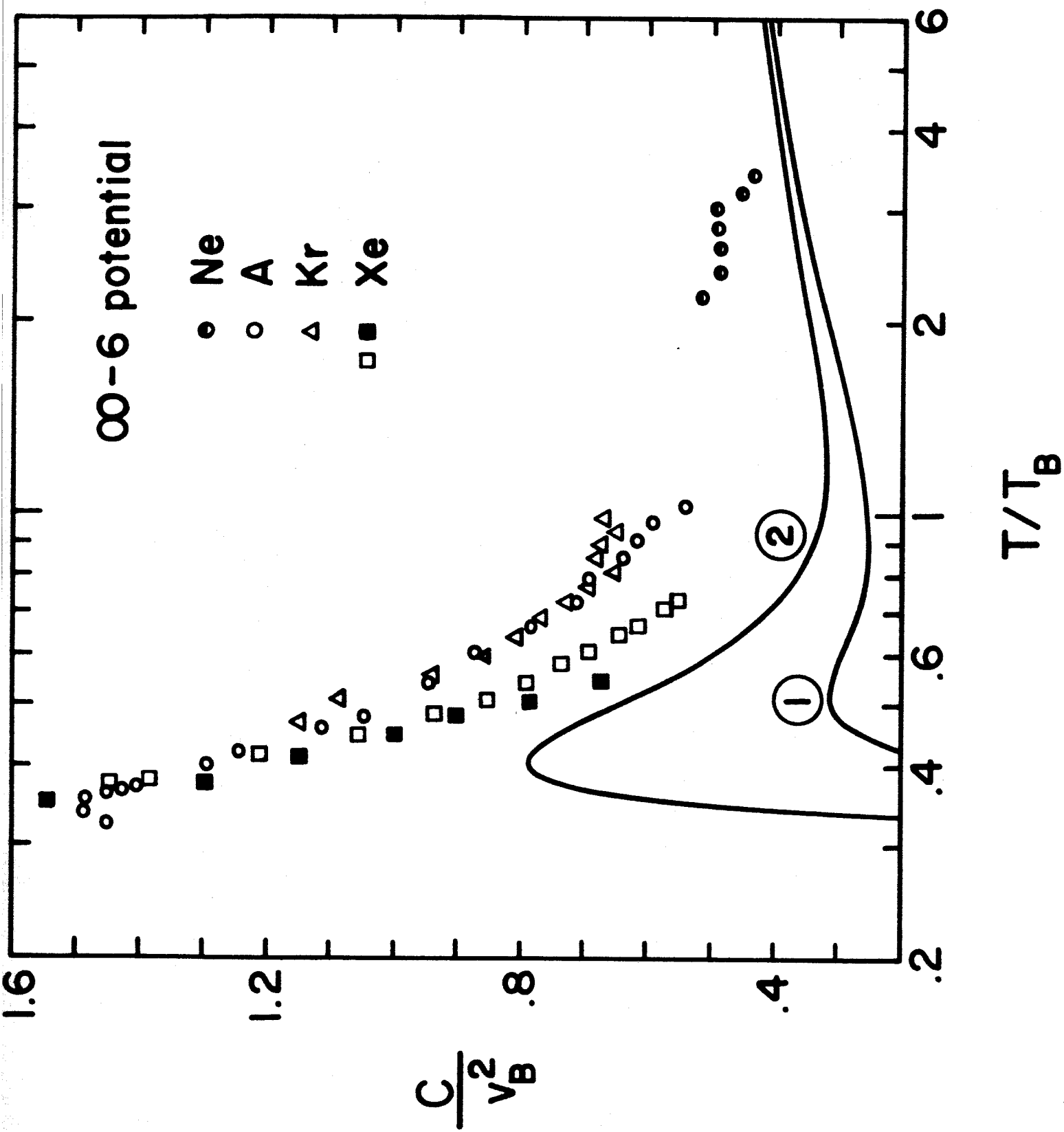


**Fig. 11 - Reduced third virial coefficient for the  
 $\infty - 6$  potential.**

**Curve 1: Pairwise additive**

**Curve 2: Additive plus dispersion non-  
additivity**

**Experimental points as in Fig. 7**



## REFERENCES

- 1 F. O. Rice and E. Teller, The Structure of Matter (John Wiley and Sons, Inc., 1949), Chap.8.
- 2 B. M. Axilrod and E. Teller, J. Chem. Phys. 11, 299 (1943); B. M. Axilrod, J. Chem. Phys. 17, 1349(1949); 19, 719(1951).
- 3 Y. Muto, Nippon Suugaku-Buturigakkwai Kizi 17, 629(1943); as reported by Y. Midzuno and T. Kihara, J. Phys. Soc. Japan 11, 1045(1956) and by T. Kihara, Adv. Chem. Phys. 1, 267(1958).
- 4 W. L. Bade, J. Chem. Phys. 27, 1280(1957).
- 5 B. Linder and D. Hoernschemeyer, J. Chem. Phys. 40, 622(1964); B. Linder, J. Chem. Phys. 40, 2003(1964).
- 6 S. Koba, S. Kaneko, and T. Kihara, J. Phys. Soc. Japan 11, 1050(1956); T. Kihara, Adv. Chem. Phys. 1, 267(1958).
- 7 H. W. Graben and R. D. Present, Phys. Rev. Letters 9, 247 (1962).
- 8 A. E. Sherwood and J. M. Prausnitz, J. Chem. Phys. 41, 413 (1964).
- 9 J. H. Dymond, M. Rigby, and E. B. Smith, J. Chem. Phys. 42, 2801(1965).
- 10 R. Eisenschitz and F. London, Z. Physik 60, 491(1930).
- 11 H. Margenau, Phys. Rev. 56, 1000(1939).
- 12 N. Lynn, Proc. Phys. Soc. (London) 72, 201(1958).
- 13 J. O. Hirschfelder and J. W. Linnett, J. Chem. Phys. 18, 130(1950); N. Moore, J. Chem. Phys. 33, 471(1960); D. Y. Kim, Z. Physik 166, 359(1962).
- 14 L. Jansen, Phys. Rev. 125, 1798(1962).
- 15 L. Jansen, Phys. Letters 4, 91(1963); L. Jansen and S. Zimering, Phys. Letters 4, 95(1963); L. Jansen, Phys. Rev. 135, A1292 (1964).

- 16 H. W. Graben, Thesis, University of Tennessee (1962).
- 17 P. Rosen, J. Chem. Phys. 21, 1007(1953).
- 18 A. Shostak, J. Chem. Phys. 23, 1808(1955).
- 19 R. T. Mc Ginnies and L. Jansen, Phys. Rev. 101, 1301(1956).
- 20 S. F. Boys, Proc. Roy. Soc. (London) A200, 542(1950).
- 21 J. O. Hirschfelder, C. F. Curtiss, and R. B. Bird, Molecular Theory of Gases and Liquids (John Wiley and Sons, Inc., New York, 1954), Chap.13.
- 22 T. Kihara, Rev. Mod. Phys. 25, 831(1953).
- 23 (a) S. F. Boys and I. Shavitt, Proc. Roy. Soc. (London) A254, 499(1960). (b) R. J. Munn, J. Chem. Phys. 40, 1439(1964).  
(c) F. J. Smith, E. A. Mason, and R. J. Munn, J. Chem. Phys. 42, 1334(1965).